Submitted to ADVANCED MATERIALS

Polarity Switching of Charge Transport and Thermoelectricity in Self-Assembled Monolayer Devices

By *David A. Egger*, *Ferdinand Rissner*, *Egbert Zojer*, and *Georg Heimel*[*]

[*] Dr. G. Heimel, D.A. Egger
Institut für Physik
Humboldt-Universität zu Berlin
Brook-Taylor-Strasse 6, 12489 Berlin (Germany)
E-mail: georg.heimel@physik.hu-berlin.de
Prof. E. Zojer, D.A. Egger, F. Rissner
Institute of Solid State Physics
Graz University of Technology
Petersgasse 16, 8010 Graz (Austria)

Keywords: Self-Assembled Monolayer, Molecular Electronics, Charge Transport, Thermoelectricity, Density-Functional Theory.

Decreasing the size of electronic devices through top-down approaches has its intrinsic limits. Therefore, bottom-up approaches to nanoelectronics based on individual functional molecules constitute an appealing alternative in principle.[1] In practice, however, such devices are challenging to realize because contacts need to be structured down to the molecular scale as well. Compatible with current structuring techniques are devices based on self-assembled monolayers (SAMs) of organic molecules covalently linked to metallic electrodes.[2,3] There, the electrodes are laterally extended *and* charge transport occurs at the desired nanoscale across the SAM. Functionality is introduced to the device through targeted chemical design of the constituting individual molecules. Such strategies often rely on the individual molecules to maintain their intended function within the completed SAM device. This is, however, not necessarily the case,[4–7] which calls for design criteria that encompass the interrelation between individual-molecule and monolayer electrical properties.

In the present theoretical work we demonstrate that, through the collective electrostatic action of intramolecular dipoles within the SAM, already the most basic measureable quantity of an electronic device, the current at a given voltage, can be strikingly different for isomeric molecules that exhibit virtually identical frontier-orbital energies as isolated species. More importantly, the same collective electrostatic effect can even reverse the polarity of charge transport across such SAMs, *i.e.*, whether electronic transport is established *via* occupied (p-type) or unoccupied (n-type) electronic states.[8] Understanding this intriguing effect represents an important step towards establishing viable guidelines for the rational design of functional elements in future molecular electronic devices.

We chose to illustrate the consequences of aligned polar bonds in close-packed self-assembled molecular monolayers on the basis of a prototypical model system in molecular

electronics, the so-called 'Tour wire' (**Figure 1**a).[9] Both in single-molecule and SAM devices, Tour wires have been frequently functionalized by chemical substitution at the central ring as indicated in Figure 1b, *e.g.*, dipoles introduced by polar amino and/or nitro groups have been suggested to lead to negative differential resistance,[10] switching,[11] and rectification.[12] However, such side groups might detrimentally affect the close packing and high degree of order observed in SAMs of unsubstituted Tour wires.[13] Therefore, also alternative chemical design strategies have been pursued to imbue molecular wires with electrical dipole moments. For instance, fluorination of one of the terminal phenyl rings in Tour-wire based systems[14,15] or distributing dipoles[16] within the backbone of oligo(*para*-phenylene)s has been seen to trigger molecular-level switching and/or diode behavior in respective single-molecule junctions.[17] Here, we explore a conceptually different approach. Specifically, we built chemical modifications directly into the molecular backbone by *symmetrically* replacing the two outermost phenyl rings of a Tour wire with pyrimidine rings, resulting in the N_{in} molecule (Figure 1c). Note that, other than in the aforementioned strategies for chemical design,[9–12,14–17] N_{in} has no net dipole moment. Rather, polar bonds within the pyrimidine units and on the thiol anchoring groups add up to local dipole moments at both 'ends' of the molecule (arrows in Figure 1c). In contrast previous studies,[18,19] where changing the anchoring groups from thiols to isocyanines has been observed to reverse the polarity of charge transport through SAMs, we compare N_{in} to its equally thiolated isomer N_{out} (Figure 1d). There, local pyrimidine and S-H dipoles point in opposite directions on both ends of the molecule and, consequently, both the local and the net molecular dipole moments are essentially zero. Importantly, we calculated the highest occupied and lowest unoccupied fully delocalized π-orbitals (see Supporting Information) to be only ~ 0.1 eV higher in energy for the isolated N_{in} molecule than for N_{out}. As the alignment of these highest occupied (HOTC) and lowest unoccupied end-to-end transport channels (LUTC) with the Fermi level,

E_F, of external electrodes has emerged as a dominant parameter controlling current flow through molecular junctions,[2,20] one might expect equally similar electrical characteristics of N_{in} and N_{out}.

To compare the charge-transport properties of these two species, we sandwiched SAMs of N_{in} and N_{out} between two gold electrodes (Figure 1e) and performed density-functional theory (DFT) based electronic structure[21,22] and transport calculations.[23] The result of this procedure is the transmission function, T(E), which describes the 'probability' for an electron impinging on the device from out of one electrode at a certain energy E to be transmitted through the SAM into the other electrode. Current-voltage (I-V) characteristics were then evaluated using:[20]

$$\mathrm{I(V)} = \frac{2\mathrm{e}}{h}\int dE\left[f(\mathrm{E}-\mu_{\mathrm{left}}) - f\left(\mathrm{E}-\mu_{\mathrm{right}}\right)\right]\mathrm{T(E)}, \qquad (1)$$

where $f(x)$ is the Fermi-Dirac occupation function (at 300 K unless otherwise noted) and $\mu_{\mathrm{left,right}} = \mathrm{E_F}\pm\mathrm{e}\frac{\mathrm{V}}{2}$ with e the elementary charge. The reader is referred to the Experimental Section for details on the system setup and the computational methodology; a critical assessment of the employed level of theory (briefly summarized also at the end of this communication) is given in the Supporting Information.

The calculated I-V curves for the N_{in} and N_{out} SAMs are shown in Figure 1f (thick lines). Despite the fact that the frontier transport-channel energies of the isolated molecules are very similar, we find pronounced differences between the two monolayers: For the N_{in} SAM, the current is up to a factor of 9 (at 1.4 V) higher in the low-bias regime; in fact, the applied bias

voltage would have to be ~ 0.4 V higher to arrive at a comparable current through the N_{out} SAM. Note that this difference is not related to the (small) energy difference between the respective orbitals in the isolated molecules (~ 0.1 eV). Just to illustrate this, we shifted the transmission curves 0.05 eV down for the N_{in} and 0.05 eV up for the N_{out} SAM and re-calculated the I-V curves *via* Eq. (1). The difference between the two systems is fully conserved (Figure 1f, thin lines).

However, the fact that the I-V curves of N_{in} and N_{out} devices shift in the *same* direction upon shifting the transmission curves in *opposite* directions already presages the fundamentally different nature of charge transport through the SAMs, which becomes more apparent when the current through occupied and unoccupied states is calculated separately; technically, this is achieved by setting $T(E) = 0$ for $E > E_F$ and $T(E) = 0$ for $E < E_F$, respectively, and re-evaluating Eq. (1). The results in **Figure 2**a show that N_{in} SAMs primarily conduct *via* occupied (p-type), and N_{out} SAMs primarily *via* unoccupied (n-type) channels. It has been theoretically proposed[8] that such a change in the polarity of charge-transport from p-type to n-type should be experimentally accessible through the thermoelectric properties of the SAMs. This has recently been demonstrated by heating the substrate supporting the molecular monolayers and measuring thermoelectricity with the conductive tip of a scanning-tunneling[18,24,25] or atomic-force microscope.[26] To provide a thusly testable prediction for the present systems, we calculated the thermoelectric current by imposing zero bias voltage, *i.e.*, by setting V=0 in Eq. (1), and continuously varying the temperatures of the two contacts, which enter Eq. (1) through the broadening of the respective Fermi functions. Indeed, upon applying a temperature gradient across the SAMs, the direction of charge flow is reversed between N_{in} and N_{out} (Figure 2b). Accordingly, the Seebeck coefficients, extracted from our

calculated zero-bias transmission functions as ~ +17 μV/K for the N_{in} and ~ -15 μV/K for the N_{out} SAMs, are of opposite sign.

These charge-transport characteristics naturally originate in the relative energetic alignment of the molecular transport channels and E_F in the completed devices. To understand the above-described differences between N_{in} and N_{out}, we thus compare the corresponding transmission functions in **Figure 3**a and realize that, other than in the free molecules, corresponding transport channels of the two SAMs now differ in energy by ~ 0.7 eV; as T(E) is intimately related to the density of states (see Supporting Information), this relative shift would be experimentally testable by photoelectron spectroscopy on N_{in} and N_{out} SAMs adsorbed on conducting substrates. An important consequence of the difference in energy-level alignment is that the channel closest to E_F, which determines transport polarity, is the HOTC for N_{in} and the LUTC for N_{out}. Moreover, the onset of transmission is ~ 0.2 eV closer to E_F for N_{in} (dotted lines). As, in the (symmetric) systems considered here, half of the applied voltage drops between the Fermi energy of each electrode and the SAM conduction channels, the bias has to be increased by ~ 2 × 0.2 = 0.4 eV for N_{out} to attain a total current comparable to that through N_{in}, which translates into the voltage difference of ~ 0.4 V highlighted in Figure 1f.

Furthermore, T(E) dictates[8,18,24–26] the observed sign of the thermocurrent (Figure 3b): Applying different temperatures to the contacts changes the width of their respective Fermi-Dirac electron occupation functions. N_{in} SAMs provide a transport channel (the HOTC) at an energy below E_F, where the concentration of electrons is higher on the cold electrode, thus driving them towards the hot electrode (p-type). In contrast, N_{out} provides a transmission pathway (the LUTC) at an energy above E_F, where electrons are driven from hot to cold (n-type).

In search for the origin of the qualitative differences between the transmission functions of the two systems, we first computed the step in the potential energy, ΔE_{BD}, which arises from the interfacial charge re-arrangements associated with SAM-Au bond formation and which shifts all monolayer electronic states relative to E_F (for details see Ref. [27]). Due to the different positions of the nitrogens, ΔE_{BD} is indeed different for N_{in} and N_{out} (Figure 3c). While the origin of this difference might be a potentially interesting detail by itself, we refer the reader to Ref. [28] for a discussion of these interfacial 'bond dipoles' as well as their impact on energy-level alignment, and focus here on the remarkable fact that, in contrast to Refs. [18,25,26], it is of the wrong sign to explain the observed differences in the alignment of the frontier conduction channels with E_F: starting from the (almost) identical situation in the free molecules, the electronic states of N_{in} are apparently shifted *down more* in energy (by $\delta \sim 0.4$ eV) relative to E_F than those of N_{out}. And yet, in the SAM device, the transport channels of N_{in} are *higher* in energy (by *ca.* 0.7 eV) with respect to E_F than those of N_{out} (Figure 3a).

This implies that, in contrast to the situation for isolated molecules, the energies of both HOTC and LUTC have to differ substantially between N_{in} and N_{out} SAMs already prior to contact with the metallic leads. To test this hypothesis, we calculated the electronic structure of the respective free-standing monolayers (*i.e.*, without gold electrodes), where sulfurs are saturated with hydrogens. Indeed, we find the transport channels in the N_{in} monolayer to be ~ 1.1 eV closer to the vacuum level, E_{vac}, than those of N_{out} (see Supporting Information). This appreciable difference can be understood on the basis of the local dipoles indicated in Figures 1c and 1d.[29] For N_{in}, SAM formation corresponds to arranging the local net dipoles at each end of the individual molecules (Figure 1c) into surface dipole layers on both sides of the monolayer.[29] We emphasize that, as they are located entirely on the organic part of the

SAM device, they act independently of and in addition to well-understood metal/organic interface effects already captured by ΔE_{BD}.[27,30] These *all-organic surface dipole layers* create steps in the potential energy (**Figure 4**, left center panel), which lift the entire potential-energy landscape around the molecular backbones and, with it, the transport channels towards E_{vac} (compare left top and bottom panels). In contrast, for N_{out}, the local pyrimidine and thiol dipoles almost perfectly cancel on both ends of the molecule (Figure 1d) and, thus, induce only minor modifications to the potential-energy landscape upon SAM formation (right panels in Figure 4). As discussed above, the resulting difference in HOTC and LUTC energies between the free-standing N_{in} and N_{out} monolayers is subsequently mitigated by the binding of the SAMs to the electrodes, where the transport channels of N_{in} are shifted down more with respect to E_F by $\delta \sim 0.4$ eV (Figure 3c). This then results in the final situation (Figure 3a) with the transport channels of N_{in} lying higher in energy by *ca.* 1.1 - 0.4 = 0.7 eV than those of N_{out}, the HOTC of N_{in} being closer to E_F than the LUTC of N_{out} and, in particular, the different polarity of charge transport and thermoelectric current through the N_{in} and N_{out} SAMs. The purely electrostatic origin of the effect just described underlines its fundamental nature[31] and additional results on systems following the same design principle of local dipoles introduced *via* polar bonds confirm that it is by no means limited to the N_{in}/N_{out} pair of molecules (see Supporting Information **Figure S3**).

In a final note we remark that, because it originates in polar bonds within the SAMs themselves, the effect just explained should, in principle, be independent of details in the local S-Au docking geometry.[32] Also, we briefly comment on the potential impact of shortcomings in the applied computational methodology: While in the Supporting Information we explicitly show that the choice of the DFT functional is inconsequential, it is well established that the Kohn-Sham gap underestimates the transport gap of (organic)

semiconductors and that (semi-)local approximations to the exchange-correlation functional cannot capture polarization-induced reductions of the gap.[33] However, as also demonstrated in the Supporting Information, the observed polarity switch between N_{in} and N_{out} persists as long as potential upwards corrections to the DFT-calculated LUTC energies do not exceed potential downwards corrections to the HOTC energies by more than ~ 0.6 eV. Even in case they did, however, the collective electrostatic action of intramolecular dipoles would still give rise to an even more pronounced and equally unexpected difference in the total current through N_{in} and N_{out} SAMs.

In summary, two isomeric molecules with essentially identical energies of their frontier delocalized π-orbitals were found to result in two SAM devices with substantially different charge-transport characteristics: The total current in the low-bias regime differs by up to one order of magnitude and the polarity of charge transport through the SAMs switches from p- to n-type, entailing a reversal in the sign of the thermoelectric current and, thereby, of the Seebeck coefficient. These observations are rationalized through the formation of organic surface dipole layers as individual molecules comprising polar bonds are assembled into close-packed SAMs. Our present study thus highlights the collective electrostatic action of deliberately introduced polar bonds on the periphery of otherwise non-polar molecules as a new strategy for controlling device functionality beyond altering molecular dipole moments and anchoring chemistry. It clearly shows that understanding materials properties at the molecular level is of undisputed relevance, but remains far from sufficient for predicting the behavior of more complex systems, such as assemblies of molecules in a monolayer-based electronic device. It is stressed here that the consideration of collective effects is an essential prerequisite for the rational design of functional elements in future molecular electronic circuits.

Experimental

To isolate the effect of the molecular chemical structure on charge transport through the SAMs, we exploited the inherent advantages of a computational approach, namely, that extrinsic influences can conveniently be controlled. In particular, we disregarded potential reconstructions of the gold surface[32] and chose a co-facial[34] over a possible herringbone[13] molecular packing; methylene spacers between the thiol and the pyrimidine units (Figures 1c and 1d) are introduced to reduce the electronic coupling between metal contacts and the molecular cores, thus preserving their intrinsic electronic structure in a SAM device and suppressing the potential impact of molecular orientation on transport characteristics.[35] All species were optimized in gas-phase and assembled into 2D-periodic monolayers without further geometry relaxation. The monolayers were then sandwiched between two (111)-terminated gold electrodes with one molecule per p(2×2) surface unit-cell (Figure 1e, area per molecule 30.2 $Å^2$). Sulfur-gold bonding was assumed to proceed through cleavage of the thiols' hydrogens and the sulfur adsorption site was predetermined in a separate calculation of methylthiolate on Au(111).

Our study relies on DFT using the gradient-corrected exchange-correlation (XC) functional of Perdew, Burke, and Ernzerhof.[36] Geometry optimizations (force cutoff 0.01 eV/Å) of the isolated molecules and electronic-structure calculations of free-standing 2D-periodic monolayers (8×8 $k_{||}$-points) were performed with the VASP code[21] using the projector augmented-wave method[37] and a plane-wave cutoff of 20 Ryd. To solve the electronic scattering problem, we extracted the Hamiltonian and overlap matrices from a SIESTA[22] calculation on bulk gold in a (2×2×√6) supercell (8×8×6 k-points, double-ζ polarized atomic-orbital basis set). Recursive Green's function techniques[23,38] were then employed to compute

the self-energies, $\Sigma_{\mathrm{left,right}}$, of the leads.[23] The (zero-bias) transmission function $\mathrm{T(E)}$ was subsequently obtained as:

$$\mathrm{T(E)} = \sum_{\mathrm{k_{||}}} \mathrm{w_{k_{||}}} \cdot \mathrm{Tr}\left[\Gamma_{\mathrm{left}} \mathrm{G_D} \Gamma_{\mathrm{right}} \mathrm{G_D^{\dagger}}\right] \quad (2)$$

with

$$\Gamma_{\mathrm{left,right}} = i\left[\Sigma_{\mathrm{left,right}} - \Sigma^{\dagger}_{\mathrm{left,right}}\right] \quad (3)$$

and $\mathrm{G_D}$ the retarded Green's function of the device region (comprising the SAM and 6 layers of gold as shown in Figure 1e) extracted from a second SIESTA calculation (8×8 $\mathrm{k_{||}}$-points with weights $\mathrm{w_{k_{||}}}$).[23] All computational parameters were well converged as benchmarked in Ref. [39].

Finally, current-voltage (I-V) characteristics were evaluated using Eq. (1) and Seebeck coefficients, S, were obtained as:[8]

$$\mathrm{S} = \frac{-\pi^2 k_B^2 T}{3|\mathrm{e}|} \frac{1}{\mathrm{T(E)}} \frac{\partial \mathrm{T(E)}}{\partial \mathrm{E}}\Big|_{\mathrm{E=E_F}}, \quad (4)$$

where k_B is the Boltzmann constant, T is the average temperature of the device (300 K) and e is the charge of an electron. Note that, in general, the transmission function $\mathrm{T(E)} = \mathrm{T(E,V)}$, but neglecting the bias dependence has been shown to have only a minor impact at the relatively low voltages considered here.[40] 3D-representations of the systems were generated with XCrysDen.[41]

Acknowledgements
The authors thank L. Beverina, A.M. Kelterer, C. Slugovc, and S. Hecht for helpful discussions. D.A.E. is a recipient of a DOC scholarship by the Austrian Academy of Sciences. Financial support by the Austrian Science Fund (FWF): P20972-N20 and the Integrative Research Institute for the Sciences (IRIS) Adlershof is gratefully acknowledged.

Submitted to ADVANCED MATERIALS

Received: ((will be filled in by the editorial staff))
Revised: ((will be filled in by the editorial staff))
Published online: ((will be filled in by the editorial staff))

[1] H. Song, M. A. Reed, T. Lee, *Adv. Mater.* **2011**, *23*, 1583–1608.
[2] H. B. Akkerman, P. W. M. Blom, D. M. de Leeuw, B. de Boer, *Nature* **2006**, *441*, 69–72.
[3] A. J. Kronemeijer, H. B. Akkerman, T. Kudernac, B. J. van Wees, B. L. Feringa, P. W. M. Blom, B. de Boer, *Adv. Mater.* **2008**, *20*, 1467–1473.
[4] Y. Selzer, L. Cai, M. A. Cabassi, Y. Yao, J. M. Tour, T. S. Mayer, D. L. Allara, *Nano Lett.* **2005**, *5*, 61–65.
[5] A. Landau, L. Kronik, A. Nitzan, *J. Comp. Theor. Nanosci.* **2008**, *5*, 535-544.
[6] M. G. Reuter, G. C. Solomon, T. Hansen, T. Seideman, M. A. Ratner, *J. Phys. Chem. Lett.* **2011**, *2*, 1667–1671.
[7] M. G. Reuter, T. Seideman, M. A. Ratner, *Nano Lett.* **2011**, *11*, 4693–4696.
[8] M. Paulsson, S. Datta, *Phys. Rev. B* **2003**, *67*, 241403R.
[9] L. A. Bumm, J. J. Arnold, M. T. Cygan, T. D. Dunbar, T. P. Burgin, L. Jones, D. L. Allara, J. M. Tour, P. S. Weiss, *Science* **1996**, *271*, 1705–1707.
[10] J. Chen, M. A. Reed, A. M. Rawlett, J. M. Tour, *Science* **1999**, *286*, 1550–1552.
[11] Z. J. Donhauser, *Science* **2001**, *292*, 2303–2307.
[12] F.-R. F. Fan, Y. Yao, L. Cai, L. Cheng, J. M. Tour, A. J. Bard, *J. Am. Chem. Soc.* **2004**, *126*, 4035–4042.
[13] A.-A. Dhirani, R. W. Zehner, R. P. Hsung, P. Guyot-Sionnest, L. R. Sita, *J. Am. Chem. Soc.* **1996**, *118*, 3319–3320.
[14] M. Elbing, R. Ochs, M. Koentopp, M. Fischer, C. von Hänisch, F. Weigend, F. Evers, H. B. Weber, M. Mayor, *Proc. Natl. Acad. Sci.* **2005**, *102*, 8815–8820.
[15] P. A. Lewis, C. E. Inman, F. Maya, J. M. Tour, J. E. Hutchison, P. S. Weiss, *J. Am. Chem. Soc.* **2005**, *127*, 17421–17426.
[16] D. A. Egger, F. Rissner, G. M. Rangger, O. T. Hofmann, L. Wittwer, G. Heimel, E. Zojer, *Phys. Chem. Chem. Phys.* **2010**, *12*, 4291.
[17] I. Díez-Pérez, J. Hihath, Y. Lee, L. Yu, L. Adamska, M. A. Kozhushner, I. I. Oleynik, N. Tao, *Nature Chem.* **2009**, *1*, 635–641.
[18] K. Baheti, J. A. Malen, P. Doak, P. Reddy, S.-Y. Jang, T. D. Tilley, A. Majumdar, R. A. Segalman, *Nano Lett.* **2008**, *8*, 715–719.
[19] C. D. Zangmeister, J. M. Beebe, J. Naciri, J. G. Kushmerick, R. D. van Zee, *Small* **2008**, *4*, 1143–1147.
[20] Y. Xue, S. Datta, M. A. Ratner, *J. Chem. Phys.* **2001**, *115*, 4292.
[21] G. Kresse, J. Furthmüller, *Phys. Rev. B* **1996**, *54*, 11169–11186.
[22] J. M. Soler, E. Artacho, J. D. Gale, A. García, J. Junquera, P. Ordejón, D. Sánchez-Portal, *J. Phys.: Condens. Matter* **2002**, *14*, 2745–2779.
[23] M. Nardelli, *Phys. Rev. B* **1999**, *60*, 7828–7833.
[24] P. Reddy, S.-Y. Jang, R. A. Segalman, A. Majumdar, *Science* **2007**, *315*, 1568–1571.
[25] J. R. Widawsky, P. Darancet, J. B. Neaton, L. Venkataraman, *Nano Lett.* **2012**, *12*, 354–358.
[26] A. Tan, J. Balachandran, S. Sadat, V. Gavini, B. D. Dunietz, S.-Y. Jang, P. Reddy, *J. Am. Chem. Soc.* **2011**, *133*, 8838–8841.
[27] G. Heimel, F. Rissner, E. Zojer, *Adv. Mater.* **2010**, *22*, 2494–2513.
[28] G. Heimel, L. Romaner, E. Zojer, J.-L. Brédas, *Nano Lett.* **2007**, *7*, 932–940.
[29] G. Heimel, I. Salzmann, S. Duhm, N. Koch, *Chem. Mater.* **2011**, *23*, 359–377.
[30] O. L. A. Monti, M. P. Steele, *Phys. Chem. Chem. Phys.* **2010**, *12*, 12390.
[31] A. Natan, L. Kronik, H. Haick, R. T. Tung, *Adv. Mater.* **2007**, *19*, 4103–4117.
[32] C. Vericat, M. E. Vela, G. Benitez, P. Carro, R. C. Salvarezza, *Chem. Soc. Rev.* **2010**, *39*, 1805.

[33] J. M. Garcia-Lastra, C. Rostgaard, A. Rubio, K. S. Thygesen, *Phys. Rev. B* **2009**, *80*, 245427.
[34] S. Sek, *Langmuir* **2009**, *25*, 13488–13492.
[35] I. Diez-Perez, J. Hihath, T. Hines, Z.-S. Wang, G. Zhou, K. Müllen, N. Tao, *Nature Nanotechn.* **2011**, *6*, 226–231.
[36] J. P. Perdew, K. Burke, M. Ernzerhof, *Phys. Rev. Lett.* **1996**, *77*, 3865–3868.
[37] G. Kresse, D. Joubert, *Phys. Rev. B* **1999**, *59*, 1758–1775.
[38] M. P. L. Sancho, J. M. L. Sancho, J. M. L. Sancho, J. Rubio, *J. Phys. F: Met. Phys.* **1985**, *15*, 851–858.
[39] M. Strange, I. S. Kristensen, K. S. Thygesen, K. W. Jacobsen, *J. Chem. Phys.* **2008**, *128*, 114714.
[40] Y. Xue, M. Ratner, *Phys. Rev. B* **2003**, *68*, 115406.
[41] A. Kokalj, *Comput. Mater. Sci.* **2003**, *28*, 155.

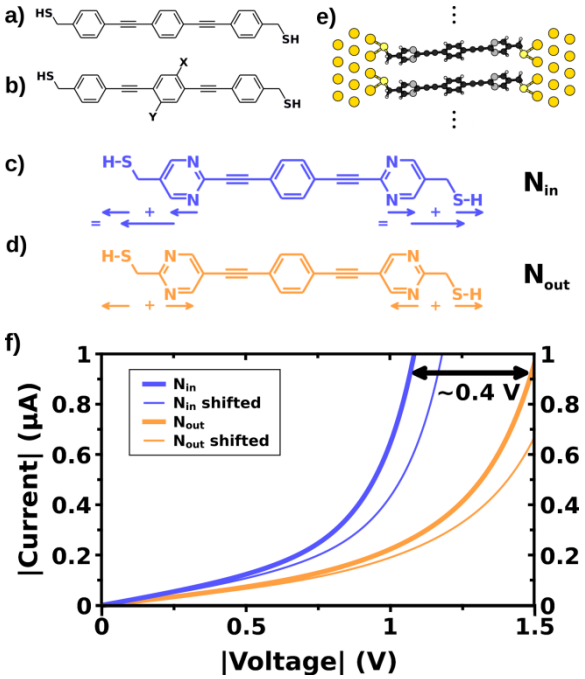

Figure 1. (a) Unsubstituted and (b) substituted Tour wire. (c) N_{in} and (d) N_{out} molecules with arrows indicating local dipoles. (e) Side view of the N_{in} SAM-device structure. (f) Calculated current-voltage characteristics of the SAM devices; thin lines were computed from shifted transmission functions (see text for details). The current is reported per unit cell (area 30.2 $Å^2$) containing one molecule.

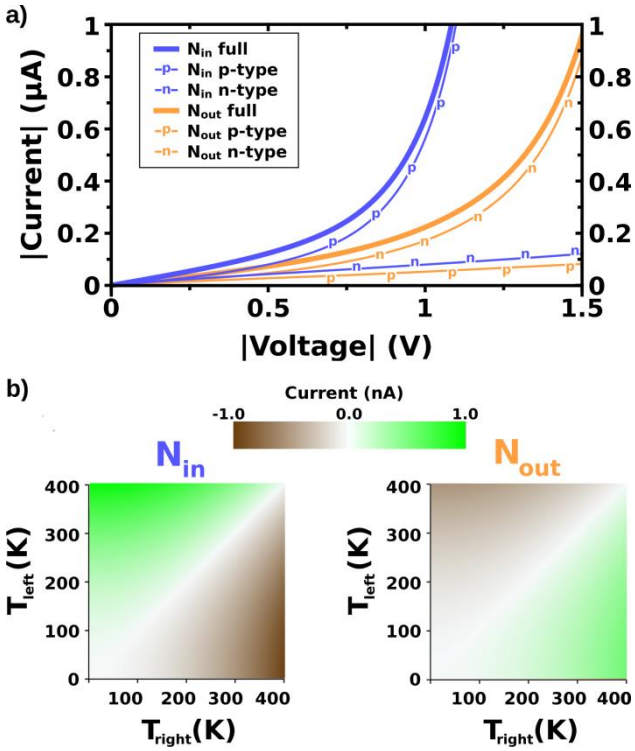

Figure 2. (a) Calculated current through occupied ('p') and unoccupied states ('n'); thick lines indicate the total current from Figure 1f. (b) Thermoelectric current calculated for the N_{in} and N_{out} monolayers (see text for details). A positive current signifies a flow of electrons from right to left.

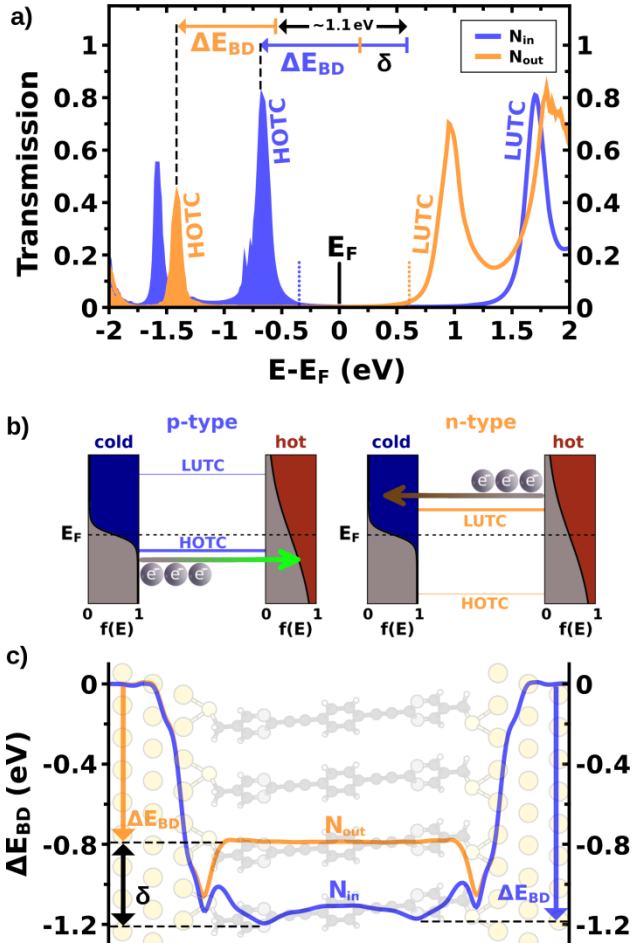

Figure 3. (a) Calculated transmission functions for the N_{in} and N_{out} SAM devices; the Fermi level, E_F, is set as zero. HOTC denotes the highest occupied and LUTC the lowest unoccupied transmission channels; dotted lines indicate the respective onsets. (b) Cartoons showing how contacts of different temperature, due to different Fermi-Dirac occupations, $f(E)$, give rise to thermocurrent of opposite sign through N_{in} (left) and N_{out} (right) SAM devices. (c) Interfacial potential-energy steps, ΔE_{BD}, arising from metal/SAM bonding and the difference, δ, between ΔE_{BD} of N_{in} and N_{out}; these quantities are also indicated in (a).

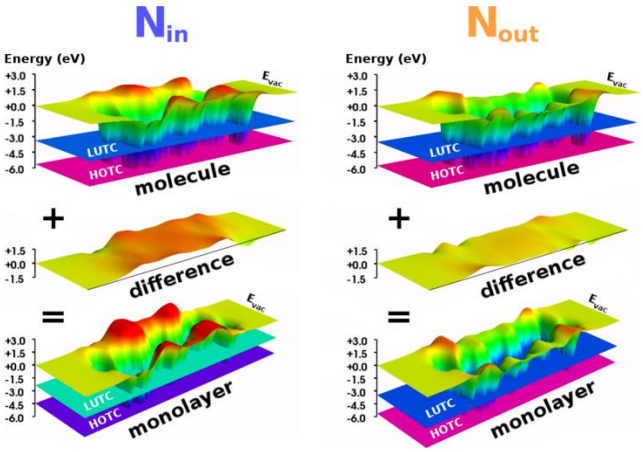

Figure 4. (top) DFT-calculated potential-energy wells and energies of the highest occupied (HOTC) and lowest unoccupied (LUTC) end-to-end delocalized π-orbitals relative to the vacuum level, E_{vac}, for the isolated N_{in} and N_{out} molecules. (center) Potential-energy differences arising upon assembly of the individual molecules into the respective SAMs. (bottom) Potential-energy wells and HOTC/LUTC energies of the respective SAMs.

Self-assembled monolayer devices can exhibit drastically different charge-transport characteristics and thermoelectric properties despite being composed of isomeric molecules with essentially identical frontier-orbital energies. This is rationalized by the cooperative electrostatic action of local intramolecular dipoles in otherwise nonpolar species, thus revealing new challenges but also new opportunities for the targeted design of functional building blocks in future nanoelectronics.

Keywords: Self-Assembled Monolayer, Molecular Electronics, Charge Transport, Thermoelectricity, Density-Functional Theory.

David A. Egger, Ferdinand Rissner, Egbert Zojer, and Georg Heimel*

Polarity Switching of Charge Transport and Thermoelectricity in Self-Assembled Monolayer Devices